Eur Radiol (2014) 24:2810–2818
DOI 10.1007/s00330-014-3322-7

FORENSIC MEDICINE

Post-mortem cardiac diffusion tensor imaging: detection of myocardial infarction and remodeling of myofiber architecture

Sebastian Winklhofer · Christian T. Stoeck · Nicole Berger · Michael Thali · Robert Manka · Sebastian Kozerke · Hatem Alkadhi · Paul Stolzmann

Received: 22 December 2013 / Revised: 24 June 2014 / Accepted: 7 July 2014 / Published online: 24 July 2014

Abstract
Objectives To investigate the accuracy of post-mortem diffusion tensor imaging (DTI) for the detection of myocardial infarction (MI) and to demonstrate the feasibility of helix angle (HA) calculation to study remodelling of myofibre architecture.
Methods Cardiac DTI was performed in 26 deceased subjects prior to autopsy for medicolegal reasons. Fractional anisotropy (FA) and mean diffusivity (MD) were determined. Accuracy was calculated on per-segment (AHA classification), per-territory, and per-patient basis, with pathology as reference standard. HAs were calculated and compared between healthy segments and those with MI.
Results Autopsy demonstrated MI in 61/440 segments (13.9 %) in 12/26 deceased subjects. Healthy myocardial segments had significantly higher FA ($p<0.01$) and lower MD ($p<0.001$) compared to segments with MI. Multivariate logistic regression demonstrated that FA ($p<0.10$) and MD ($p=0.01$) with the covariate post-mortem time ($p<0.01$) predicted MI with an accuracy of 0.73. Analysis of HA distribution demonstrated remodelling of myofibre architecture, with significant differences between healthy segments and segments with chronic ($p<0.001$) but not with acute MI ($p>0.05$).
Conclusions Post-mortem cardiac DTI enablesdifferentiation between healthy and infarcted myocardial segments by means of FA and MD. HA assessment allows for the demonstration of remodelling of myofibre architecture following chronic MI.
Key Points
- *DTI enables post-mortem detection of myocardial infarction with good accuracy.*
- *A decrease in right-handed helical fibre indicates myofibre remodelling following chronic myocardial infarction.*
- *DTI allows for ruling out myocardial infarction by means of FA.*
- *Post-mortem DTI may represent a valuable screening tool in forensic investigations.*

Keywords Magnetic resonance imaging (MeSH) · Diffusion tensor imaging · Myocardial infarction · Ventricular remodelling · Autopsy

Abbreviations

CI	Confidence interval
DTI	Diffusion tensor imaging
FA	Fractional anisotropy
HA	Helix angle
HE	Hematoxylin and eosin
ICC	Intraclass correlation coefficients
MD	Mean diffusivity
MI	Myocardial infarction
MRI	Magnetic resonance imaging
NPV	Negative predictive value
PD	Proton density
PPV	Positive predictive value
ROC	Receiver operating characteristics
ROI	Region of interest

S. Winklhofer · N. Berger · R. Manka · H. Alkadhi · P. Stolzmann (✉)
Institute of Diagnostic and Interventional Radiology, University Hospital Zurich, Raemistrasse 100, 8091 Zurich, Switzerland
e-mail: paul.stolzmann@usz.ch

S. Winklhofer · N. Berger · M. Thali · P. Stolzmann
Department of Forensic Medicine and Radiology, Institute of Forensic Medicine, University of Zurich, Zurich, Switzerland

C. T. Stoeck · R. Manka · S. Kozerke
Institute for Biomedical Engineering University and ETH Zurich, Zurich, Switzerland

R. Manka
Clinic for Cardiology, University Hospital Zurich, Zurich, Switzerland

Introduction

Ischemic heart disease accounts for approximately 10 % of annual deaths worldwide, with myocardial infarction (MI) representing the leading cause of mortality [1]. Acute MI results in alterations of myocardial tissue integrity, whereas chronic MI is associated with remodelling of the myofibre architecture in the later course of disease [2].

Diffusion tensor imaging (DTI) has recently emerged as a non-invasive method for evaluating tissue integrity and myofibre architecture [2–4]. DTI visualizes cardiac fibre architecture [2] and allows for the detection of structural changes in the arrangement of cardiac fibres associated with MI [3]. As such, DTI provides additional information over conventional magnetic resonance imaging (MRI) techniques.

Water molecules diffuse rapidly in the direction aligned with the intact myofibres, but slowly across them [5]. Different parameters can be derived from measuring the diffusion in different directions. The estimated tensors include mean diffusivity (MD), fractional anisotropy (FA), and helix angles (HA). FA is thought to represent a sensitive marker for tissue integrity, as demonstrated in neuronal axons and validated histologically, whereas MD indicates the diffusivity of water molecules and reflects the redistribution of intracellular and extracellular space volumes [2]. HA analyses by MRI were developed in cardiac imaging primarily to enable better demonstration and improved understanding of the helical fibre orientation and architecture of the myocardium [6].

In the living, alterations of myocardial tissue integrity caused by MI have been shown to result in increased MD and reduced FA in both acute and chronic MI, while remodelling led to decreased HA in chronic MI [2]. In forensic science, the need for perpetual and objective forensic documentation of findings triggered a rising demand for non-invasive imaging [7]. More specifically, conventional MRI exploiting T1, T2, and proton density (PD)-weighted imaging contrast enabled the detection of myocardial oedema and haemorrhage after MI [8, 9]. Although the applicability of cardiac DTI to MRI has been investigated [10–12], its diagnostic performance has not yet been systematically studied for the detection of MI in post-mortem studies.

The objective of this study was to investigate the accuracy of post-mortem DTI for the detection of acute and chronic MI and to demonstrate the feasibility of HA in the study of chronic remodelling of myofibre architecture.

Materials and methods

This study was approved by our institutional review board and the public prosecution office. Informed consent was not applicable due to the post-mortem nature of the study.

Study population

Between 2012 and 2013, a total of 40 consecutive medicolegal cases scheduled for conventional autopsy were prospectively enrolled. Inclusion criteria were age over 18 years and either positive history of ischemic heart disease or at least three positive risk factors for coronary artery disease. Exclusion criteria were deformations of the thorax (n=1), severe chest trauma (n=3), penetrating trauma to the heart or aorta (n=2), and advanced decomposition (n=8) [13].

The post-mortem time interval was defined as the time between death and MRI as determined by forensic investigation. A total of 26 deceased subjects (eight women, 54± 15 years, range 22–85 years) were included in the study (Table 1).

MRI data acquisition and image reconstruction

Data acquisition was performed on a 3 Tesla whole-body MRI (Achieva 3.0 T, Philips Healthcare, Best, Netherlands), with all hearts in situ and without fixation. A 16-channel phased-array coil (SENSE XL, Philips Healthcare) was used for signal reception. A diffusion-weighted multi-slice spin echo sequence with single-shot echo planar imaging readout was used, with the following parameters: TR/TE, 5662/60 ms; flip angle, 90°; voxel size, 1.50/1.50/1.50 mm; signal averages, 6. Parallel imaging with twofold under-sampling and sensitivity encoded image reconstruction was applied [14]. Stejskal–Tanner diffusion encoding was applied in 15 directions distributed on the unit sphere, with a b-value of 1,200 s/mm^2 [15]. The effective duration of the diffusion gradients was

Table 1 Demographics of deceased and autopsy findings

Total number of deceased	26
Mean age±SD (years)	54±15
Females (n)	8 (31 %)
Body weight±SD (kg)	81±15
Height±SD (cm)	174±8
Body mass index±SD (kg/m^2)	26.6±4.4
Cases with myocardial infarctions (n)	
• Total	12 (46 %)
• Acute	5 (19 %)
• Chronic	5 (19 %)
• Both	2 (8 %)
Cause of death as determined by final legal report (n)	
• Cardiovascular failure	19 (73 %)
• Intoxication	3 (12 %)
• Asphyxia	2 (7 %)
• Metabolic disease	1 (4 %)
• Other/unknown	1 (4 %)

12.4 ms per lobe, and the diffusion time was 12.1 ms. Readout duration and echo time was shortened by using a rectangular field of view, applying slice excitation angulated with respect to the refocusing slab and thereby avoiding signal attenuation from previous excitations at different slice positions [16]. A 3D whole-heart acquisition using a T2 contrast-prepared multi-shot gradient echo sequence was acquired directly afterward as an anatomical reference.

FA and MD maps were reconstructed in all cases on a standard MRI workstation (ViewForum; Philips, Best, Netherlands). After estimation of the diffusion tensors, myofibre tractography using Runge–Kutta integration [17, 18] was performed in five of the 26 cases (19 %). Only tensors within the compact left ventricular myocardium were considered for processing. The helix angle was defined as the angle between the short axis image plane and the projection of the first eigenvector onto the epicardial tangent plane, spanned by the local circumferential vector and the image plane normal [19].

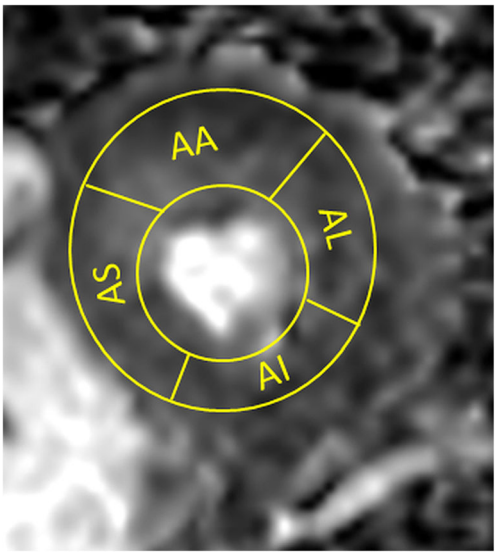

Fig. 1 Schematic demonstration of region of interest (ROI) placement in the left ventricle according to American Heart Association segmentation model, demonstrating four segments in short axis apical slice on fractional anisotropy map. Clockwise: AS, anterior; AL, lateral; AI, inferior; AS, septal segment

Image analysis

One reader, blinded to the history of the deceased, assessed the image quality of each DTI data set using a four-point Likert scale scoring system: 1, good image quality without any artefacts; 2, good image quality with minor chemical shift artefacts; 3, major chemical shift artefacts; and 4, major distortion of left ventricular geometry hindering generation of FA and MD maps. Score 4 was considered as non-diagnostic image quality.

Two radiologists (four and eight years of experience with cardiac MRI), who were blinded to patient data, results from autopsy, and other imaging studies, independently measured FA and MD by placing regions of interest (ROIs). ROIs completely encircled each of the left ventricular myocardial segments. Placement carefully avoided endocardial and pericardial contours (Fig. 1). Segments were defined according to the standardized myocardial segmentation scheme as suggested by the American Heart Association (AHA), in which the myocardium and the left ventricular cavity is divided into 17 segments (i.e., six basal segments, six midventricular segments, four apical segments, and the apex) [20].

Autopsy

Autopsies were performed within 24 hours after MRI by board-certified forensic pathologists (7–30 years of experience), assisted by forensic pathology residents and mortuary technicians, in line with standardized forensic autopsy procedures. The myocardium was cut in base parallel slices from the mitral valve to the apex to allow for segmentation of the left myocardium according to the standardized 17-segment AHA model [20]. Matching of segments between forensic and radiological macroscopic examinations was performed by means of macroscopic description. Heart specimens were photographically documented. Additional histopathology was performed in all cases with macroscopic lesions suspicious for MI. Analyses included chromotrope-aniline-blue, elastic van Gieson, hematoxylin, and eosin (HE) staining protocols. Evaluation was performed to differentiate between healthy and infarcted myocardium, with subdivisions of acute and chronic MI. Acute MI was characterized by increased eosinophilia, wavy fibres, oedema, contraction bands, and myocardial haemorrhage, whereas the presence of collagenous scaring, fibrocytes, and hypertrophic adjacent fibres were indicative of chronic MI [8].

Statistical analysis

Categorical variables were expressed as frequencies and percentages; continuous variables were expressed as mean±standard deviation (range). Testing for normality was performed using the Shapiro–Wilk test.

The inter-reader and intra-reader agreements regarding FA and MD values for myocardial segments were analysed using intraclass correlation coefficients (ICCs). ICC values of 0.61–0.80 were interpreted as substantial, and 0.81–1.00 as excellent.

An unpaired two-tailed Student's T-test was used to compare FA and MD between healthy and infarcted myocardial segments. One-way analysis of variances (ANOVA) was used with the post hoc Fisher's Least Significant Difference (LSD) procedure to compare FA and MD between healthy myocardial segments and segments with acute and chronic MI.

We performed multivariate logistic regression analyses with a forward entry (entry $p<0.05$, removal $p>0.10$) to predict segments with MI by FA and MD. In a second step, the same model was calculated but also included post-mortem time intervals. The model performance was evaluated using c-statistics and comparing with a Z-test.

Receiver operating characteristic (ROC) analysis was performed analysing FA and MD in relation to MI. Areas under the curve (AUC), sensitivity, specificity, positive predictive value (PPV), and negative predictive value (NPV) were calculated from Chi-Square tests of contingency for optimal cutoff values derived from ROC analysis. Analyses were carried out on a per-segment (n=440, i.e., 17 segments in 26 cases minus 2 apical segments which were missed), per-territory (n=78; i.e., segments assigned to standard supply of the left anterior descending coronary artery, segments 1, 2, 7, 8, 13, and 14; left circumflex coronary artery, segments 5, 6, 11, 12, and 16; and right coronary artery, segments 3, 4, 9, 10, and 15 [20]), and per-case basis. A generalized estimating equation was applied for per-segment analyses to account for clustering of myocardial segments within vascular territories and patients.

Autopsy was used as reference standard. Respective 95 % confidence intervals (CI) were calculated from binomial expression for ROC and segmental analysis.

Student's T-test for independent samples was used to compare HA distribution between segments with MI and healthy myocardial segments at the same level (i.e., basal, midventricular, apical) in opposite locations (e.g., anterior vs. posterior).

A p value <0.05 was used to indicate statistical significance. All statistical analyses were performed using commercially available software (SPSS, release 21.0, Chicago, IL, USA).

Results

Autopsy demonstrated MI in 61/440 segments (13.9 %) in 12/26 cases (46 %) (*see* Table 1). Of these 61 segments with MI, acute MI was identified in 26/61 segments (43 %) and chronic MI was found in 35 segments (57 %) in a total of 25/78 territories (i.e., at least one segment with MI identified per territory; 32 %). The mean post-mortem time interval between death and MRI was 19±11 hours (range, 4–48 hours).

Image quality of DTI was scored 1 in 10/26 (38 %), 2 in 10 (38 %), and 3 in six (23 %) cases. None of the 26 studies was of non-diagnostic image quality; all data sets allowed for the generation of FA and MD maps. However, the apex of the left ventricle was not imaged in 2/26 cases (8 %) due to malpositioning of imaging volume.

Intra-reader agreement was excellent for FA (ICC=0.99, $p<0.001$) and for MD (ICC=0.97, p<0.001). The inter-reader agreement was also excellent for FA (ICC=0.96, $p<0.001$) and for MD (ICC=0.92, $p<0.001$).

Regarding healthy myocardial segments without MI, mean FA and MD were 0.37±0.08 and 0.61±0.15×10^{-3} mm^2/s, respectively. In myocardial segments with MI, mean FA and MD were 0.34±0.06 and 0.68±0.14×10^{-3} mm^2/s, respectively (Fig. 2). Healthy myocardial segments demonstrated significantly higher FA ($p<0.01$) and lower MD ($p<0.001$) compared to segments with MI (*see* Fig. 2). FA and MD did not differ significantly between segments with acute and chronic MI (FA acute 0.34±0.06 and chronic 0.33±0.06×10^{-3} mm^2/s, $p=0.92$; MD acute 0.69±0.15 and chronic 0.67±0.14×10^{-3} mm^2/s, $p=0.73$) (Fig. 3). Multivariate logistic regression demonstrated that both FA ($p<0.10$; coefficient -4.5±2.4, β=0.01) and MD ($p=0.02$; coefficient 2.5±1.1; β=12.77) predicted myocardial segments with MI. C-statistics was marginal (c=0.65). Regarding the second model, multivariate logistic regression demonstrated all FA ($p<0.10$; coefficient 6.2±2.5, β=0.002), MD ($p=0.01$; coefficient 2.8±1.1; β=16.19), and post-mortem time intervals ($p<0.01$; coefficient -0.06±0.02, β=0.95) to independently predict myocardial segments with MI. C-statistics indicated good model fit, with significantly ($p<0.05$) improved c-statistics equalling 0.73.

ROC analysis demonstrated significant (both, $p<0.05$) AUCs for FA (AUC=0.38; 95 % CI, 0.31–0.45) and MD (AUC=0.63; 95 % CI, 0.56–0.71) for the differentiation between healthy and myocardial segments with MI. The best cutoff values for the detection of segments with MI were <0.36 and >0.62×10^{-3} mm^2/s for FA and MD, respectively.

Applying the aforementioned cutoff values to performance analysis on a per-segment basis, sensitivity, specificity, PPV, and NPV of FA were 64 % (95 % CI, 0.51–0.76), 50 % (95 % CI, 0.449–0.553), 17 % (95 % CI, 0.13–0.23), and 90 % (95 % CI, 0.85–0.93). On a per-territory and per-case basis, sensitivity, specificity, PPV, and NPV were 96 %, 17 %, 35 %, and 90 %, and 100 %, 7 %, 48 %%, and 100 %, respectively.

Regarding the performance of MD on a per-segment basis, sensitivity, specificity, PPV, and NPV of FA were 64 % (95 % CI, 0.51–0.76), 50 % (95 % CI, 0.449–0.553), 17 % (95 % CI, 0.13–0.23), and 90 % (95 % CI, 0.85–0.93). On a per-territory and per-case basis, sensitivity, specificity, PPV, and NPV were 68 %, 40 %, 35 %, and 72 %, and 75 %, 29 %, 47 %%, and 57 %, respectively.

The effect of clustering was not significant (both, $p>0.05$), and therefore justified the assumption that the segments could be analysed independently.

Fibre tracking was performed in nine deceased subjects. We investigated two deceased subjects with healthy myocardial segments, five with chronic MI, and two with acute MI. Joint histograms demonstrated differences in HA distribution between healthy myocardial segments and segments with chronic MI (Fig. 4). In chronic MI only, joint histogram of

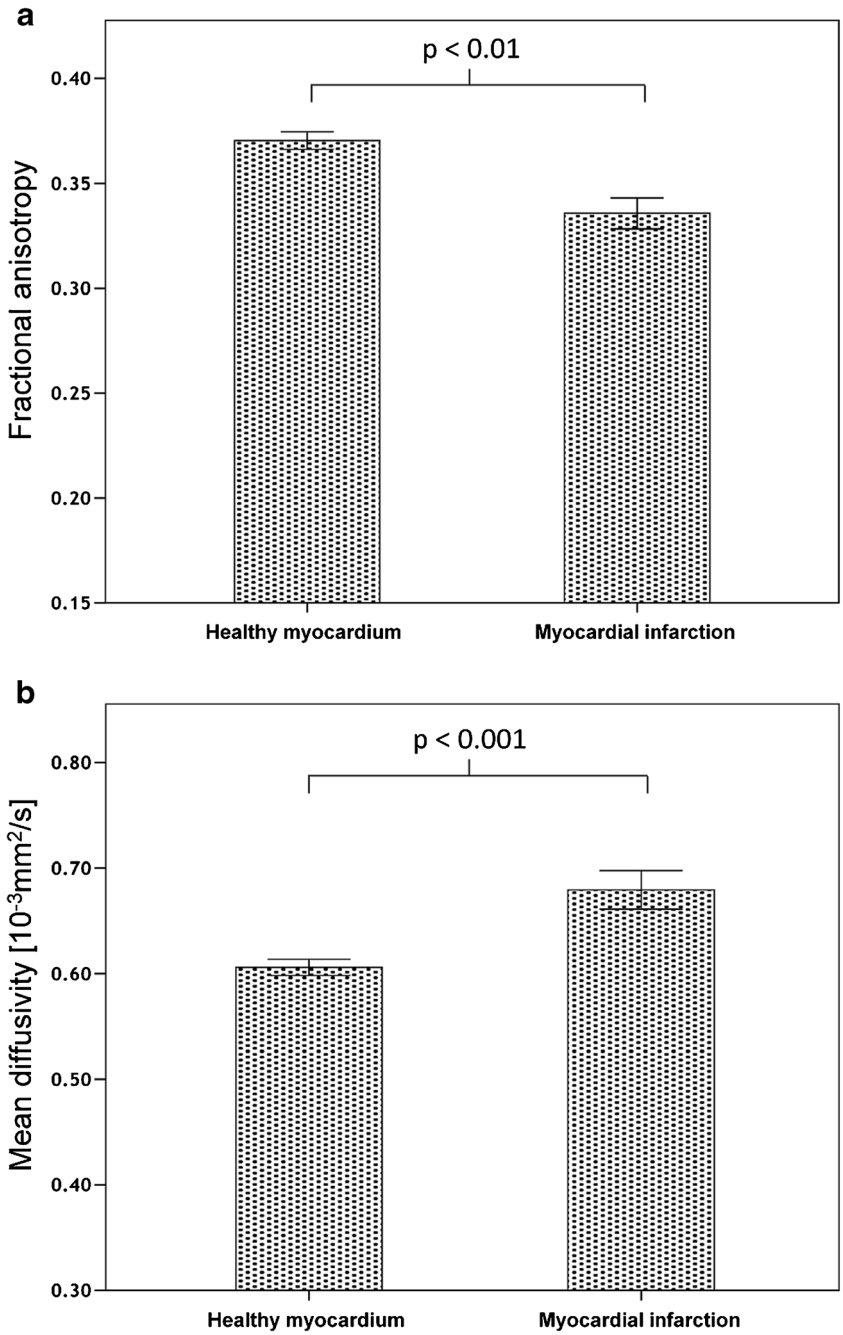

Fig. 2 Bar charts demonstrating significant differences for (**a**) fractional anisotropy and (**b**) diffusivity between healthy myocardium and myocardial segments after myocardial infarction as confirmed by pathology

the HA demonstrated remodelling of myofibre architecture resulting in a decrease of mean HA, predominantly in subendocardial locations. When considering endocardial fibres, HA was larger by 21±8° (all pairwise, $p<0.05$) in myocardial segments without evidence of MI compared to segments with MI (i.e., decrease of right-handed fibres). When comparing HA distribution, significant differences were evident between healthy and chronically infarcted myocardial segments (all pairwise, $p<0.001$) but not in myocardia with acute MI (all, $p>0.05$).

Discussion

Post-mortem MRI is being implemented in an increasing number of forensic institutions as a supplemental tool in daily routine [7]. The transfer of knowledge from established clinical imaging processes to forensic radiology, however, requires an understanding of the usefulness and applicability of techniques for post-mortem imaging [21]. With regard to clinical MRI, DTI has been applied to almost all organs in numerous scientific studies. Clinically, it is most commonly

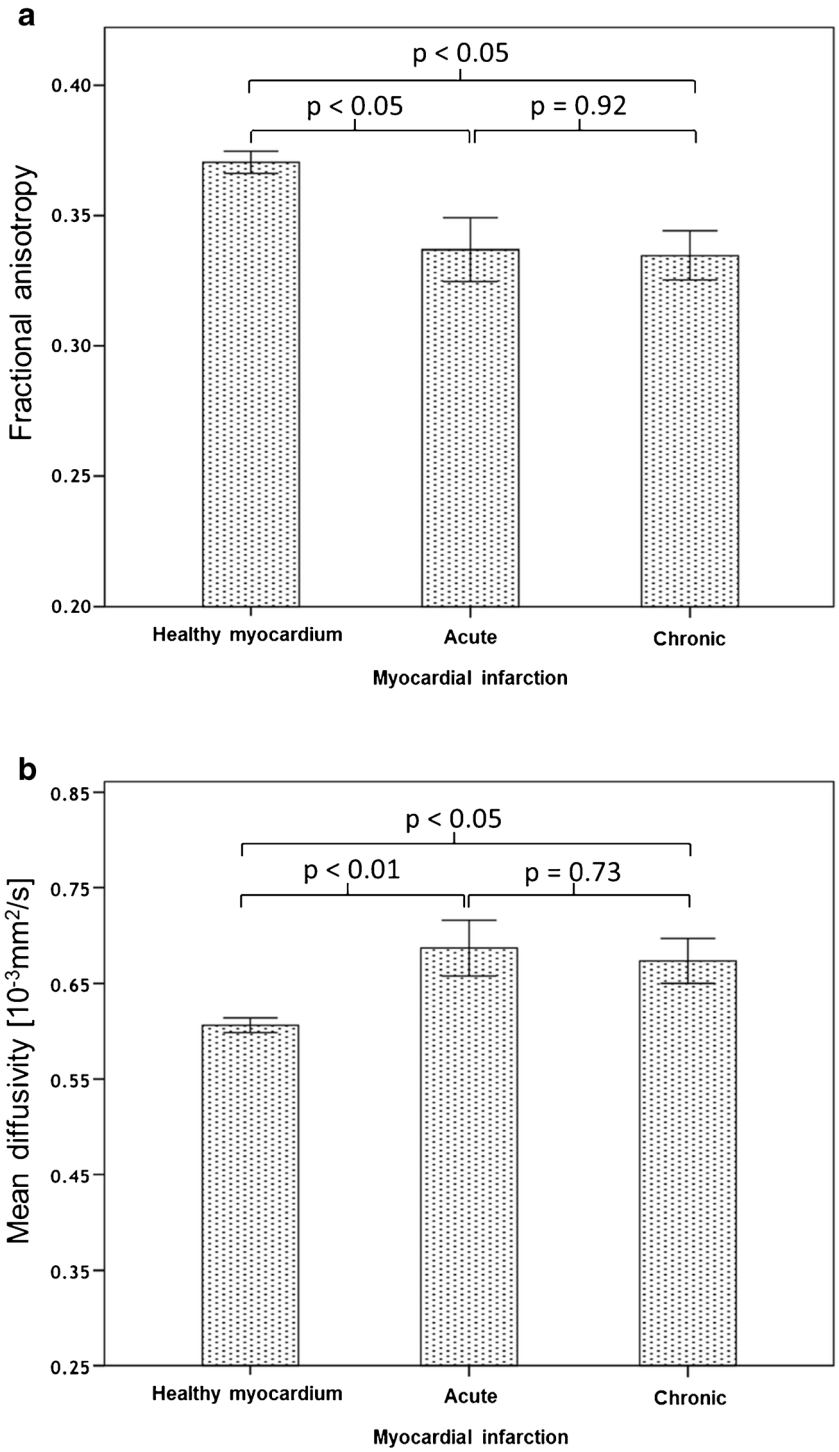

Fig. 3 Bar charts demonstrating significant differences in (**a**) fractional anisotropy and (**b**) diffusivity between both healthy myocardial segments and acute as well as chronic myocardial infarctions. Neither fractional anisotropy nor mean diffusivity differed significantly between acute and chronic myocardial infarctions

used in neuroimaging and for planning and navigation of complex surgery [22]. With regard to cardiac DTI, for a long period of time, the motion of the beating heart hampered a closer investigation of the myocardium. With novel methods such as ECG triggering or navigation with respiratory motion compensation, the reduction of artefacts has enabled in vivo cardiac DTI [23]. Post-mortem imaging carries the advantage of motion-free data acquisition, otherwise one of the major sources of artefacts in vivo DTI [5].

Our study demonstrates the ability of post-mortem DTI to detect MI by means of significantly lower FA and higher MD as compared to healthy myocardial segments. These results are in line with previous studies demonstrating the feasibility of DTI for differentiation between healthy myocardial

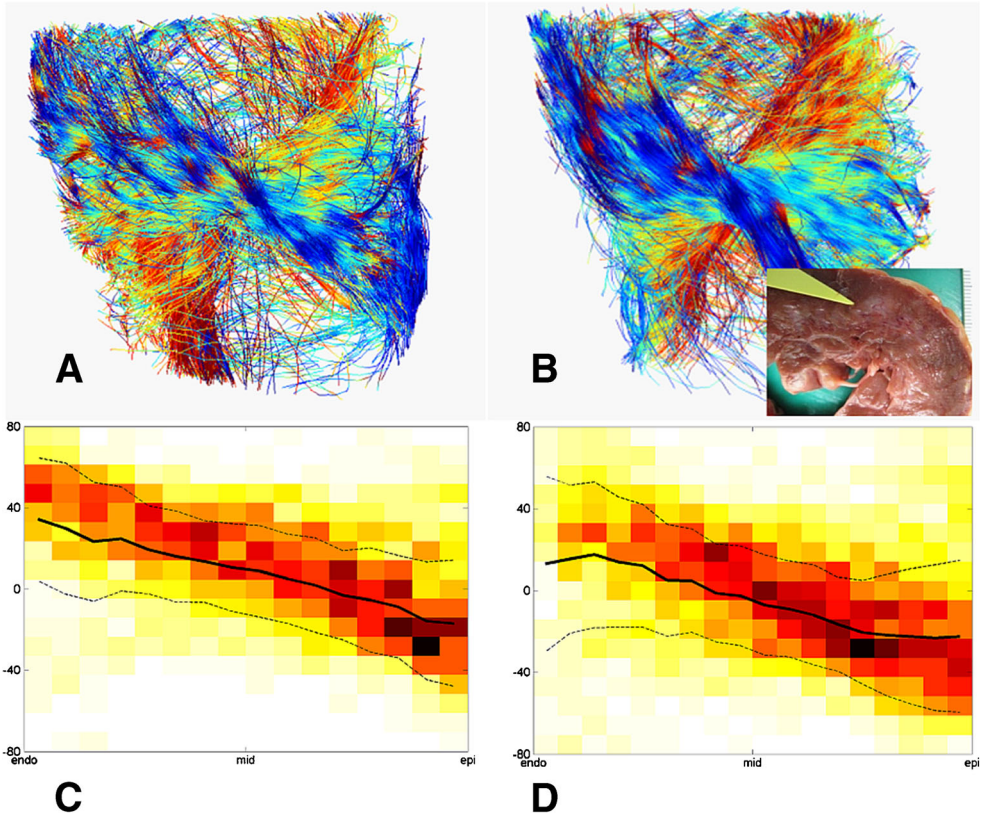

Fig. 4 Tractography of myofibre architecture (**a**) in a healthy myocardial segment and (**b**) in a segment with chronic myocardial infarction in the anterolateral wall of the left ventricle at the midventricular level, as confirmed by autopsy (*arrow, insert* **b**). Helix angles defined as the angle between the main eigenvector and the transmural short-axis plane are tagged and colour-coded. Joint histogram of the helix angles with respect to the transmural depth demonstrate (**c**) normal variations between +60 degrees at the endocardium to -40 degrees at the epicardium in healthy myocardial segments. (**d**) After chronic infarction in a corresponding myocardial segment, joint histogram of the helix angles clearly visualizes remodelling of myofibre architecture resulting in a decrease of mean helix angles in predominantly subendocardial locations

segments and segments with MI in animals and living humans [4, 24]. Values are of the same order of magnitude for both healthy segments and those with MI. Although post-mortem FA is approximately one-fourth larger than in vivo measurements in humans, differences between segments with and without MI are similarly small but nevertheless significant. These findings are best explained by myocyte swelling and lengthening after MI [25]. In acute MI, the increased but less directional mobility of water molecules directly results in lower FA, as diffusion-limited boundaries are reduced as a result of ischemic cell injury. Studies have shown that FA sequentially increases while MD decreases in MI from acute to chronic states, based on the microstructural improvement of tissue integrity [2].

In our study, a similar trend was observed, particularly with regard to MD, although not reaching statistical significance. In addition, results for FA and MD are within the same order of magnitude as described in two post-mortem cases with ischemic heart disease [12]. Mean MD as observed post-mortem was approximately twice as low as that observed with in vivo DTI [2]. The most likely reason for this phenomenon is the hypothermia of the corpse during MRI [26].

Both decreased FA (<0.36) and increased MD ($>0.62\times10^{-3}$ mm^2/s) were associated with good sensitivity, whereas the NPV was higher when considering the FA parameter alone. As such, we recommend the use of both the FA and MD parameters for suspicion of MI in forensic practice, whereas an FA within the normal limits safely allows for ruling out MI. This again demonstrates that FA best represents tissue integrity. Additionally, in line with the aforementioned results, MD is more temperature-dependent than FA, which is of particular importance in post-mortem forensic scanning. The accuracy of MI prediction was significantly improved by adding post-mortem time intervals to the statistical model, which is in line with increasing MD and decreasing FA values as the post-mortem interval lengthens [10].

Knowledge of DTI measurements may shift the pathologist's attention towards a more detailed myocardial autopsy. The downside of FA and MD cutoffs is their poor specificity, although this could be offset with subsequent autopsy if DTI is regarded as a filter test. In this scenario, the additional combined use of conventional MRI may increase the low specificity of DWI alone.

A decrease in HA, predominantly in subendocardial locations, was found in segments with chronic MI. Quantitative analyses of the HA distribution demonstrated remodelling of myofibre architecture, with significant differences between healthy and chronically infarcted myocardial segments. These findings indicative of myofibre remodelling have been researched in animal and patient studies [2, 4, 27–29] but have not yet been described in post-mortem MRI.

In our study, we found significant differences between HA in chronic MI and that in healthy myocardia, but we did not encounter significant differences between HA in acute MI and

healthy myocardial segments. In contrast, Wu et al. [30] demonstrated significant differences in HA for both chronic and acute MI in comparison to healthy myocardia. The most likely reason for this discrepancy is the shorter interval of time between infarction in our study, which was less than 24 hours, as compared to the Wu et al. series, where a mean period of 22±14 days was indicated between MI and MRI in cases of acute MI.

An increase in negative HA has also been observed in the left ventricular myocardium after heart failure [31] and as a response to exercise [32]. Although we observed similar results post-mortem, it is important to note that remodelling is associated with high interindividual variability [33].

Limitations

We acknowledge the following study limitations. First, the given post-mortem time intervals may not be absolutely accurate, as they rely on forensic estimations. The tissue integrity and myofibre architecture may change as a function of time after death due to decomposition, and therefore may be a source of error. With a maximum interval of 48 hours between death and MRI, the length of time was kept as short as possible. Second, water diffusivity is related to temperature [34], and therefore we attempted to image each body at a temperature above 15 ° C to avoid relevant changes between examinations. Third, ROI measurements were placed by encircling entire myocardial segments. This may be a source of error, as microstructural alterations in the myocardium adjacent to infarcted segments cannot be excluded.

Conclusions

Post-mortem cardiac DTI allows for diagnosis of segments with MI as well as for demonstration of healthy myocardial segments, which may aid in forensic documentation and investigation planning. HA assessment enables the demonstration of infarct chronicity by evidencing remodelling of myofibre architecture with a reduction of right-handed fibres.

Acknowledgments The scientific guarantor of this publication is Paul Stolzmann. The authors of this manuscript declare no relationships with any companies whose products or services may be related to the subject matter of the article. The authors state that this work has not received any funding. One of the authors has significant statistical expertise. Institutional Review Board approval was obtained. Written informed consent was not required for this study, as informed consent was not applicable due to the post-mortem nature of the study. Methodology: prospective diagnostic or prognostic study, performed at one institution.

Conflict on interest No conflict of interest declared.

References

1. Go AS, Mozaffarian D, Roger VL et al (2013) Heart disease and stroke statistics—2013 update: a report from the American Heart Association. Circulation 127:e6–e245
2. Wu Y, Wu EX (2009) MR study of postnatal development of myocardial structure and left ventricular function. J Magn Reson Imaging 30:47–53
3. Wu Y, Zou C, Liu W et al (2013) Effect of B-value in revealing postinfarct myocardial microstructural remodeling using MR diffusion tensor imaging. Magn Reson Imaging 31:847–856
4. Chen J, Song SK, Liu W et al (2003) Remodeling of cardiac fiber structure after infarction in rats quantified with diffusion tensor MRI. Am J Physiol Heart Circ Physiol 285:H946–H954
5. Sosnovik DE, Wang R, Dai G, Reese TG, Wedeen VJ (2009) Diffusion MR tractography of the heart. J Cardiovasc Magn Reson 11:47
6. Hsu EW, Muzikant AL, Matulevicius SA, Penland RC, Henriquez CS (1998) Magnetic resonance myocardial fiber-orientation mapping with direct histological correlation. Am J Physiol 274:H1627–H1634
7. Baglivo M, Winklhofer S, Hatch GM, Ampanozi G, Thali MJ, Ruder TD (2013) The rise of forensic and post-mortem radiology—analysis of the literature between the year 2000 and 2011. J Forensic Radiol Imaging 1:3–9
8. Jackowski C, Christe A, Sonnenschein M, Aghayev E, Thali MJ (2006) Postmortem unenhanced magnetic resonance imaging of myocardial infarction in correlation to histological infarction age characterization. Eur Heart J 27:2459–2467
9. Thali MJ, Yen K, Schweitzer W et al (2003) Virtopsy, a new imaging horizon in forensic pathology: virtual autopsy by postmortem multislice computed tomography (MSCT) and magnetic resonance imaging (MRI)—a feasibility study. J Forensic Sci 48:386–403
10. Eggen MD, Swingen CM, Iaizzo PA (2012) Ex vivo diffusion tensor MRI of human hearts: relative effects of specimen decomposition. Magn Reson Med 67:1703–1709
11. Holmes AA, Scollan DF, Winslow RL (2000) Direct histological validation of diffusion tensor MRI in formaldehyde-fixed myocardium. Magn Reson Med 44:157–161
12. Crooijmans HJA, Ruder TD, Zech WD et al (2013) Feasibility of quantitative diffusion imaging of the heart in post-mortem MR. J Forensic Radiol Imaging 1:124–128
13. Levy AD, Harcke HT, Mallak CT (2010) Postmortem imaging: MDCT features of postmortem change and decomposition. Am J Forensic Med Pathol 31:12–17
14. Jaermann T, Crelier G, Pruessmann KP et al (2004) SENSE-DTI at 3T. Magn Reson Med 51:230–236
15. Dou J, Tseng WY, Reese TG, Wedeen VJ (2003) Combined diffusion and strain MRI reveals structure and function of human myocardial laminar sheets in vivo. Magn Reson Med 50:107–113
16. Wheeler-Kingshott CA, Parker GJ, Symms MR et al (2002) ADC mapping of the human optic nerve: increased resolution, coverage, and reliability with CSF-suppressed ZOOM-EPI. Magn Reson Med 47:24–31
17. Toussaint N, Stoeck CT, Schaeffter T, Kozerke S, Sermesant M, Batchelor PG (2013) In vivo human cardiac fibre architecture estimation using shape-based diffusion tensor processing. Med Image Anal 17:1243–1255
18. Fillard P, Pennec X, Arsigny V, Ayache N (2007) Clinical DT-MRI estimation, smoothing, and fiber tracking with log-Euclidean metrics. IEEE Trans Med Imaging 26:1472–1482
19. Scollan DF, Holmes A, Winslow R, Forder J (1998) Histological validation of myocardial microstructure obtained from diffusion tensor magnetic resonance imaging. Am J Physiol 275:H2308–H2318
20. Cerqueira MD, Weissman NJ, Dilsizian V et al (2002) Standardized myocardial segmentation and nomenclature for tomographic imaging

of the heart. A statement for healthcare professionals from the Cardiac Imaging Committee of the Council on Clinical Cardiology of the American Heart Association. Circulation 105:539–542
21. Roberts IS, Benamore RE, Benbow EW et al (2012) Post-mortem imaging as an alternative to autopsy in the diagnosis of adult deaths: a validation study. Lancet 379:136–142
22. Wu JS, Zhou LF, Tang WJ et al (2007) Clinical evaluation and follow-up outcome of diffusion tensor imaging-based functional neuronavigation: a prospective, controlled study in patients with gliomas involving pyramidal tracts. Neurosurgery 61:935–948, discussion 948-939
23. Nielles-Vallespin S, Mekkaoui C, Gatehouse P et al (2013) In vivo diffusion tensor MRI of the human heart: reproducibility of breath-hold and navigator-based approaches. Magn Reson Med 70:454–465
24. Wu MT, Tseng WY, Su MY et al (2006) Diffusion tensor magnetic resonance imaging mapping the fiber architecture remodeling in human myocardium after infarction: correlation with viability and wall motion. Circulation 114:1036–1045
25. Hsu EW, Xue R, Holmes A, Forder JR (1998) Delayed reduction of tissue water diffusion after myocardial ischemia. Am J Physiol 275: H697–H702
26. Le Bihan D, Delannoy J, Levin RL (1989) Temperature mapping with MR imaging of molecular diffusion: application to hyperthermia. Radiology 171:853–857
27. Healy LJ, Jiang Y, Hsu EW (2011) Quantitative comparison of myocardial fiber structure between mice, rabbit, and sheep using diffusion tensor cardiovascular magnetic resonance. J Cardiovasc Magn Reson 13:74
28. Strijkers GJ, Bouts A, Blankesteijn WM et al (2009) Diffusion tensor imaging of left ventricular remodeling in response to myocardial infarction in the mouse. NMR Biomed 22:182–190
29. Wu EX, Wu Y, Tang H et al (2007) Study of myocardial fiber pathway using magnetic resonance diffusion tensor imaging. Magn Reson Imaging 25:1048–1057
30. Wu MT, Su MY, Huang YL et al (2009) Sequential changes of myocardial microstructure in patients postmyocardial infarction by diffusion-tensor cardiac MR: correlation with left ventricular structure and function. Circ Cardiovasc Imaging 2:32–40, 36 p following 40
31. Gerdes AM, Capasso JM (1995) Structural remodeling and mechanical dysfunction of cardiac myocytes in heart failure. J Mol Cell Cardiol 27:849–856
32. Natali AJ, Wilson LA, Peckham M, Turner DL, Harrison SM, White E (2002) Different regional effects of voluntary exercise on the mechanical and electrical properties of rat ventricular myocytes. J Physiol 541:863–875
33. Kumar D, Hacker TA, Buck J et al (2005) Distinct mouse coronary anatomy and myocardial infarction consequent to ligation. Coron Artery Dis 16:41–44
34. Ruder TD, Hatch GM, Siegenthaler L et al (2012) The influence of body temperature on image contrast in post mortem MRI. Eur J Radiol 81:1366–1370